

HIGH ELECTRICAL-TO-GREEN EFFICIENCY 123 W AVERAGE-POWER QUASICONTINUOUS-WAVE LASER AT 532 nm IN COMPACT DESIGN

Menglong Li, Nan Wan, Baohua Wang, Haijuan Yu, Yingying Yang, Shilian Yan,
Wei Sun, and Xuechun Lin*

*Laboratory of All-Solid-State Laser Sources
Institute of Semiconductors, Chinese Academy of Sciences
QingHua East Road A35, Haidian District, Beijing 100083, China*

*Corresponding author e-mail: xclin@semi.ac.cn

Abstract

We present an efficient high-power quasicontinuous-wave (QCW) all-solid-state laser at 532 nm with a simple and compact symmetrical resonator. We design a stable green laser at 532 nm with an average power of 123 W and a repetition rate of 10 kHz by combining a single side-pumped Nd:YAG laser module with a type II LBO crystal for intracavity frequency doubling. The corresponding electrical-to-green conversion efficiency is 12.5%. To the best of our knowledge, this is the highest electrical-to-green efficiency in 532 nm lasers with above 100 W output power ever reported. The pulse width is 62 ns at 123 W, so the peak power is calculated up to 198.4 kW. Such a compact and efficient resonator is promising for integration into laser-application systems.

Keywords: side pumping, intracavity-frequency doubling, quasicontinuous wave, 532 nm.

1. Introduction

In recent years, high-power nanosecond green lasers have been widely used in many fields. For industry, copper welding obtained higher efficiency and reliability due to high absorptivity to green lasers [1, 2]. Also, altitude detections on the basis of Rayleigh scattering stimulated by 532 nm lasers have been applied for national defense [3]. Besides, 532 nm lasers are used to pump optical parametric oscillators for generation of new wavelengths [4]. Moreover, photoselective vaporization prostatectomy (PVP) for benign prostatic hyperplasia (BPH) can use 532 nm lasers to achieve better effect [5].

To meet the needs of system integration, the problem of how to obtain high-efficiency green-laser outputs with high power in a compact and simple resonator has received extensive attention. A green laser was reported with an average output power of 131 W in [6], 103 W in [7], and 132 W in [8]; in all these studies the use of master oscillator power amplifier (MOPA) systems with extracavity frequency doubling was made. Such schemes can achieve excellent beam quality but are characterized by complex structures and high cost.

The other method is intracavity frequency doubling. In [9], a 12 W continuous-wave single-frequency green laser was reported combining intracavity frequency doubling and diode-end pumping. A similar approach was adopted in [10] to obtain a 62 W of continuous-wave output power at 532 nm with near-diffraction-limited beam. Superior beam quality is an advantage of the end pumping, however, because

of the restriction of pump area, end pumping was not conducive to higher power. With the application of side-pumped lasers, which can help to achieve simultaneously a compact resonator and high output power, the output power of green lasers was improved gradually. For example, a 120 W average power at 532 nm and an overall wall-plug efficiency of 6.5% was reached in [11], a 138 W 532 nm laser with an electrical-to-optical efficiency of 7.9% was obtained in [12], and an average power of 180.2 W at 532 nm with an electrical-to-optical efficiency of 10.9% with one side-pumped Nd:YAG laser module was reported in [13]. All such intracavity frequency-doubling programs used dual side-pumped laser modules for high-power outputs. Taking into account all results obtained and reported, one can further optimize the efficiency and volume.

In this paper, we demonstrate an efficient high-power quasicontinuous-wave (QCW) all-solid-state laser at 532 nm with a single side-pumped Nd:YAG laser module, which can provide a 123 W average-power green laser at 10 kHz. The corresponding electrical-to-green conversion efficiency is 12.5% and the pulse width is 62 ns. To the best of our knowledge, this is the highest electrical-to-green efficiency in 532 nm lasers with above 100 W output power ever reported. Such compact and efficient resonator is promising for integration into laser-application systems.

2. Experiment Setup

The experimental setup is shown in Fig. 1. A simple symmetrical plane–plane cavity consisting of a single side-pumped laser module is used. There are five laser-diode arrays symmetrically distributed around the Nd:YAG rod (4×120 mm, with 0.6% Nd doping).

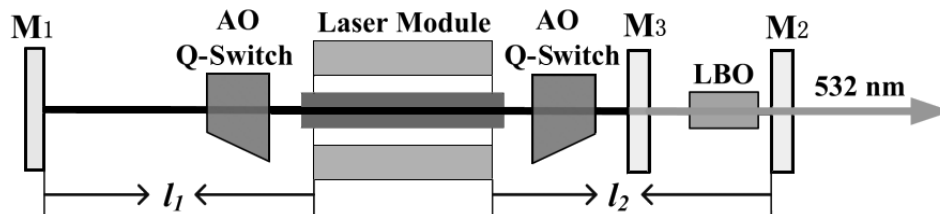


Fig. 1. Schematic of the symmetric plane–plane cavity.

Figure 2 shows the schematic of the side-pumped laser module. The rod is surrounded by a flow tube filled with cooling water, and the diode arrays are soldered to water-cooled copper sinks. When driven by a 14 A current, an input electrical power of about 980 W can produce a 490 W 808 nm laser for the pump, corresponding to an electrical-to-optical efficiency of 50%. This structure ensures a uniform distribution of the gain.

Figure 3 shows the fluorescence distribution measured by a Spiricon laser beam analyzer on the cross section of the rod at a driving current of 14 A. The approximate top-hat distribution could effectively reduce the space distortion of the oscillation beam.

As shown in Fig. 1, the cavity length is just 470 mm with $l_1 = l_2 = 170$ mm. The compactness ensures a short pulse width and low diffraction loss, and also helps to produce a miniature laser machine. Two acousto–optic (AO) Q switches were placed orthogonally with each other and close to the laser module to improve the hold-off capacity [14]. The mirror M_1 ($R > 99.8\%$ at 1,064 nm) was chosen for the total reflector, and M_2 ($R > 99.8\%$ at 1,064 nm and $T > 98.5\%$ at 532 nm) for the end dichroic mirror. The LBO crystal (4×4×20 mm³, type II phase matching at 80°C) was placed as close as possible to M_2

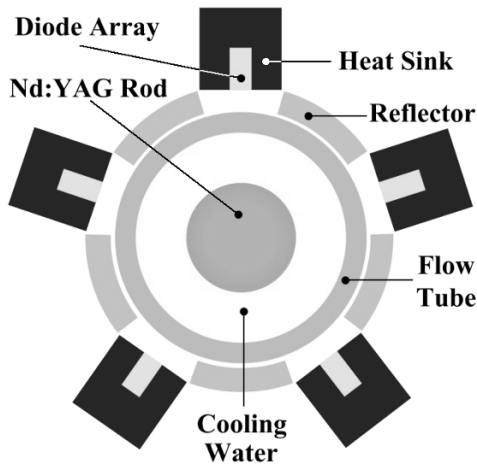


Fig. 2. Schematic of the side-pumped laser module.

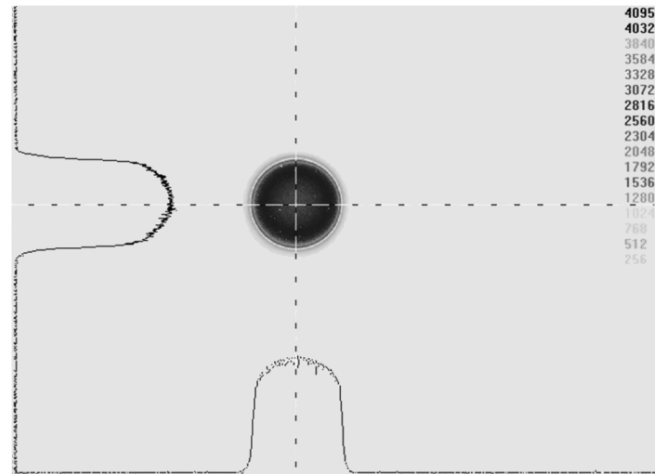


Fig. 3. Two-dimensional fluorescence distribution on the rod cross section.

to obtain a high 1,064 nm laser power density in the LBO. The AR coated at 532 nm and 1,064 nm ($T > 99.8\%$ at 1,064 nm and $T > 99.5\%$ at 532 nm), and the crystal was mounted in a copper oven with a temperature precision of $\pm 0.1^\circ\text{C}$, which directly contributed to the high stability of the second-harmonic generation (SHG). The dichroic mirror M_3 ($T > 99.8\%$ at 1,064 nm and $R > 99.5\%$ at 532 nm) was used to drive the 532 nm beam output in one direction and avoid unnecessary interference to the fundamental-frequency laser oscillation.

Using the ABCD ray propagation matrix, we calculated the beam radius of the TEM_{00} mode in the crystal and on the output mirror versus the thermal focal length; see Fig. 4. At curve 1, the change in the beam radius is not obvious before the focal length decreases to 200 mm, which contributes to a wide stable region; this is important for high and stable output. Otherwise, a radical change in the beam radius leads to decrease in the output power and deterioration of the beam quality outside the thermal-stability zone. We explored the thermal-lens effect of the crystal by measuring the equivalent thermal focal length. A nonsymmetric plane–plane cavity [15] was created at about 230 mm with an electrical current of 14 A, which met the thermal stability condition. In this point, the beam radius of the TEM_{00} mode on the output mirror was about $280\ \mu\text{m}$, which provided a sufficiently high-power density for the second-harmonic generation.

3. Experimental Results and Discussion

The average output powers of 532 nm and 1,064 nm lasers as a function of the input diode drive current are shown in Fig. 5. The 1,064 nm power was obtained using the optimum output coupler ($T = 20\%$ at 1,064 nm), replacing the end dichroic mirror M_2 , and removing the LBO crystal from the resonator. We found that the 1,064 nm laser output was 144.6 and 148 W at a repetition rate of 10 kHz, when the electrical current was 14 and 15 A, respectively. When the current exceeded 15 A, the power increase saturated because the resonator started to operate at the edge of a stable region as a result of the thermal lens effect, which corresponded to the trend shown in Fig. 4.

Through the restoration of the resonator structure shown in Fig. 1, we found that the maximum

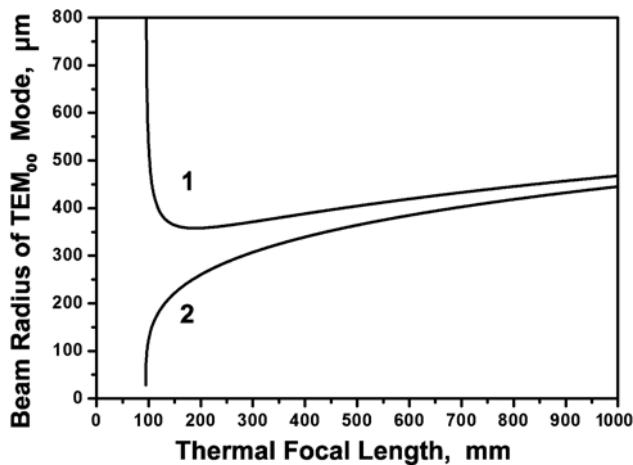


Fig. 4. Beam radius of the TEM₀₀ mode inside the crystal (curve 1) and on the output mirror (curve 2) versus the thermal focal length.

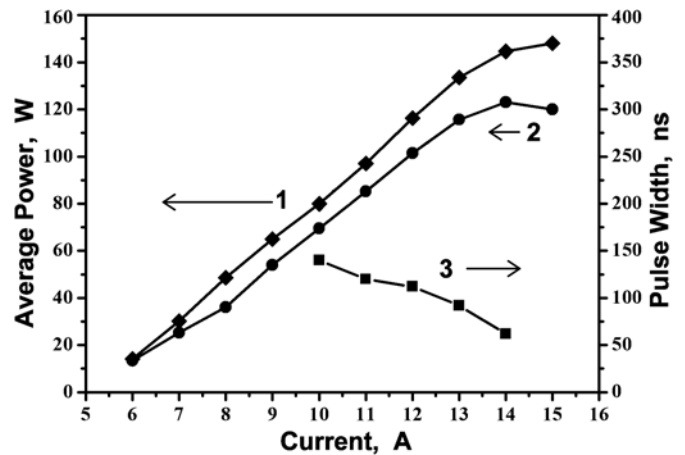


Fig. 5. Average output power at 1,064 nm (curve 1) and 532 nm (curve 2), and pulse width (curve 3) versus the diode current.

532 nm laser output was 123 W at a current of 14 A with a repetition rate of 10 kHz. The corresponding optical-to-optical efficiency and electrical-to-optical efficiency were about 25.1% and 12.5%, respectively. At a current of 15 A, the 532 nm laser power was 120 W, and the decline was also a result of the fundamental-frequency laser resonator working at the edge of a stable region.

In Fig. 5, the pulse width at 532 nm versus the diode current is shown, and we see its decrease with increase in the current. When the current was 14 A, the pulse width was 62 ns at 10 kHz, corresponding to a peak power of 198.4 kW. The pulse is shown in Fig. 6.

At an output power of 123 W, we measured the green-beam diameters with the help of a laser beam analyzer at different places along the beam-propagation direction after a focal lens ($f = 200$ mm), which was used for constructing the waist. Using the hyperbolic fitting, we estimate the beam parameter product (BPP) to be 15.5 mm·mrad. The multimode output is a result of the low spatial overlap rate

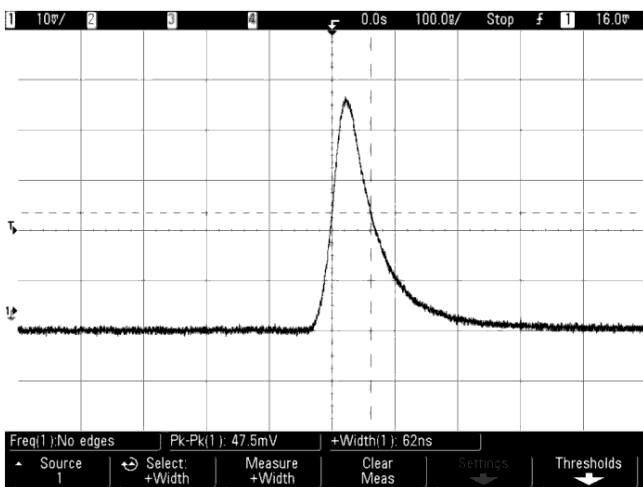


Fig. 6. A 532 nm laser pulse at 123 W.

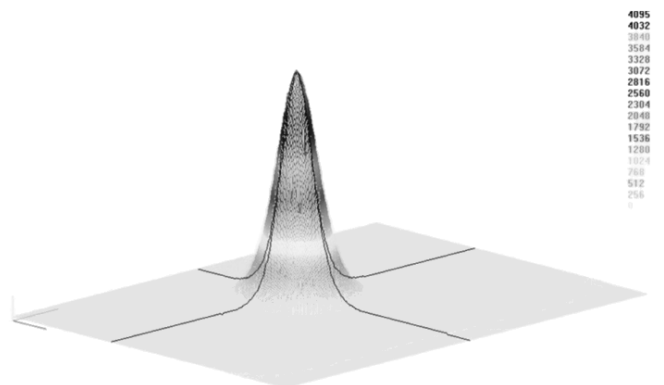


Fig. 7. Three-dimensional far-field intensity-contour distribution of the 532 nm beam at 123 W.

between the TEM₀₀ mode from the theoretical calculation shown in Fig. 4 and the pump-beam filling the whole laser crystal. Also from Fig. 4, we see that in the thermal stability zone the beam radius of the TEM₀₀ mode diminishes gradually while the current increases and thermal focal length decreases, which could cause the beam quality to degrade slightly because of the lower spatial overlap rate.

Figure 7 shows the three-dimensional far-field intensity-contour distribution of the 532 nm beam at 123 W. The far-field image was collected on the focal plane after a BK7 glass plano-convex lens ($f = 200$ mm, $\phi = 38.1$ mm, $T > 99.5\%$ at 532 nm) orthogonally placed on the optical axis at a distance 350 mm away from the output mirror. The image is a smooth intensity-distribution curve and round spot cross section, because the spatial distributions of multiple modes are mixed together on the focal plane by focusing the lens. The intensity decreases smoothly from the center to the edge, and a regular shape could meet demands for various actual applications.

In Fig. 8, we show the results of measuring the fluctuation of the output average power around 120 W. We calculate the stability using the equation

$$\pm \frac{\Delta p}{\bar{p}} = \pm \frac{(p_{\max} - p_{\min})}{2\bar{p}};$$

the stability is better than $\pm 1.1\%$ during 2.5 h. The power degradation was not observed after several hours of continuous operation, i.e., the laser is a stable and reliable system, which is a prerequisite for practical applications.

4. Conclusions

In conclusion, we have designed a high electrical-to-green efficiency QCW laser at 532 nm with high average power. Using a single side-pumped Nd:YAG laser module with a type II LBO crystal for intracavity frequency doubling, we obtained a 123 W average-power green laser at 10 kHz in a simple and compact resonator cavity. The corresponding electrical-to-green conversion efficiency is 12.5%, which is the highest electrical-to-green efficiency in 532 nm lasers with above 100 W output power ever reported. Such compact and efficient resonator is promising for integration into laser-application systems. The pulse width of the Q -switched 532 nm laser is 62 ns, corresponding to a peak power of 198.4 kW. We estimated the beam parameter product (BPP) of the green laser as 15.5 mm-mrad with the far field of a smooth intensity-distribution curve and round spot cross section. The power fluctuation over 2.5 h was calculated to be better than $\pm 1.1\%$. High-power green lasers with such excellent characteristics are appropriate for practical applications in many fields.

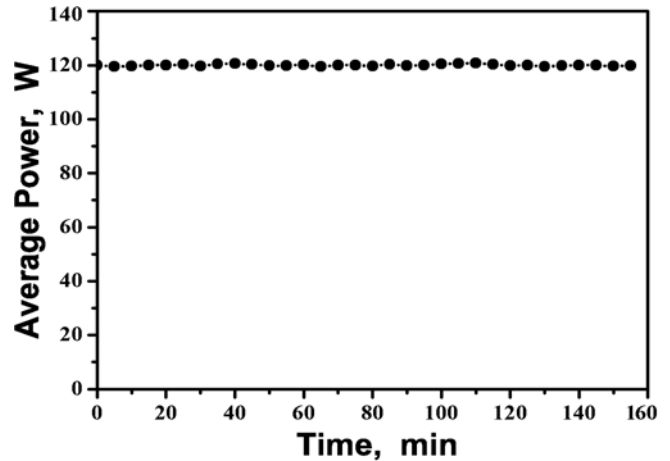


Fig. 8. Output average-power fluctuations during 2.5 h.

Acknowledgments

This research was supported by the National Key Scientific Research Project of China under Project No. 2012CB934200 and the National Natural Science Foundation of China under Projects Nos. 61205133, 51205380, 61308032, and 61308033.

References

1. A. Hess, R. Schuster, A. Heider, et al., *Physics Procedia*, **12**, 88 (2011).
2. S. Weiler, A. Hangst, C. Stolzenburg, et al., *Proc. SPIE*, **8239**, 823907 (2012).
3. X. W. Cheng, J. Song, F. Q. Li, et al., *Chin. J. Lasers*, **33**, 601 (2006).
4. T. H. My, C. Drag, and F. Bretenaker, *Opt. Lett.*, **33**, 1455 (2008).
5. M. Spaliviero, M. Araki, and C. Wong, *J. Endourol.*, **22**, 2341 (2008).
6. Y. Hirano, N. Pavel, S. Yamamoto, et al., *Opt. Commun.*, **184**, 231 (2000).
7. Q. Liu, X. P. Yan, M. L. Gong, et al., *Opt. Exp.*, **16**, 14335 (2008).
8. H. Kiriya, K. Yamakawa, T. Nagai, et al., *Opt. Lett.*, **28**, 1671 (2003).
9. H. L. Hong, L. Huang, Q. Liu, et al., *Appl. Opt.*, **51**, 323 (2012).
10. Y. F. Lü, C. L. Li, X. H. Fu, et al., *Laser Phys. Lett.*, **7**, 627 (2010).
11. S. K. Sharma, P. K. Mukhopadhyay, A. Singh, et al., *Rev. Sci. Instrum.*, **81**, 073104 (2010).
12. S. Konno, T. Kojima, S. Fujikawa, and K. Yasui, *Opt. Lett.*, **25**, 105 (2000).
13. Sh. B. Zhang, Q. J. Cui, B. Xiong, et al., *Laser Phys. Lett.*, **7**, 707 (2010).
14. Y. Bo, A. C. Geng, Y. Bi, et al., *Appl. Opt.*, **45**, 2499 (2006).
15. B. G. Zhang, J. Q. Yao, D. G. Xu, et al., *Proc. SPIE*, **4914**, 460 (2002).